
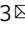


Direct *N*-substituted *N*-thiocarboxyanhydride polymerization towards polypeptoids bearing unprotected carboxyl groups

Botuo Zheng^{1,2}, Tianwen Bai², Jun Ling² [✉] & Jihong Sun^{1,3} [✉]

Synthesis of poly(α -amino acid)s bearing carboxyl groups is a critical pathway to prepare biomaterials to simulate functional proteins. The traditional approaches call for carboxyl-protected monomers to prevent degradation of monomers or wrong linkage. In this contribution, we synthesize *N*-carboxypentyl glycine *N*-thiocarboxyanhydride (CPG-NTA) and iminodiacetic acid *N*-thiocarboxyanhydride (IDA-NTA) without protection. Initiated by amines, CPG-NTA directly polymerizes into polyCPG bearing unprotected carboxyl groups with controlled molecular weight (2.8–9.3 kg mol⁻¹) and low dispersities (1.08–1.12). Block and random copolymerizations of CPG-NTA with *N*-ethyl glycine *N*-thiocarboxyanhydride (NEG-NTA) demonstrate its versatile construction of complicated polypeptoids. On the contrary, IDA-NTA transforms amines into cyclic IDA dimer-capped species with carboxyl end group in decent yields (>89%) regio-selectively. Density functional theory calculation elucidates that IDA repeating unit is prone to cyclize to be the six-membered ring product with low ΔG . The polymer is a good adhesive reagent to various materials with adhesive strength of 33–229 kPa.

¹Department of Radiology, Sir Run Run Shaw Hospital, School of Medicine, Zhejiang University, Hangzhou 310016, China. ²MOE Key Laboratory of Macromolecular Synthesis and Functionalization, Department of Polymer Science and Engineering, Zhejiang University, Hangzhou 310027, China.

³Innovation Center for Minimally Invasive Techniques and Devices, Zhejiang University, Hangzhou 310016, China. ✉email: lingjun@zju.edu.cn; sunjihong@zju.edu.cn

Functional α -amino acids play essential roles in life activities by constituting active sites of proteins and sustaining elegant architectures^{1–3}. α -Amino acids bearing carboxyl groups, such as glutamic acid and aspartic acid, attract great attention because of their reactivity, pH-responsiveness and ability to chelate metal ions^{4–6}. Scientists have made great progress in synthesizing acidic polypeptides to realize applications including self-assembly, biopharmaceutics, food industries, hydrogels and biosensors^{7–22}. Their analogs, *N*-carboxyalkyl polypeptoids, are also developed as promising building blocks for self-assembly structures and functional materials^{23–27} thanks to their excellent design flexibility and processability compared with polypeptides.

Although techniques have been developed to prepare acidic polypeptides and polypeptoids, it is still a strenuous and challenging work to introduce amino acid repeat unit with carboxyl groups into the polymer especially in the system containing a variety of functional groups²⁸. The most popular approaches are ring-opening polymerization (ROP) of α -amino acid *N*-carboxyanhydride (NCA)^{29–36} and solid phase peptide synthesis (SPPS)^{37–39}. NCAs are high reactive and able to prepare ester-protected poly(glutamic acid), poly(aspartic acid) and other polypeptides bearing inert groups with high molecular weights (MWs)^{15,40,41}. Extra steps are required to introduce intact carboxyl groups by deprotection or transformation reaction from side groups such as vinyl and thioester²⁸. The protecting benzyl ester groups also suffer from the risk of aminolysis by amine end groups⁴². Although SPPS does well in synthesizing sequence-defined poly(α -amino acid)s containing carboxyl group, it can only be carried out in milligram scales³⁷, and esterification protection of carboxyl side group is also necessary^{24,25} to prevent its wrong amidation with propagating amine group. In traditional ways, the tedious deprotection and post-modification steps take scientists great effort and time in design and purification leading to loss of products.

α -Amino acids *N*-thiocarboxyanhydrides (NTAs) are more stable monomers than NCAs^{43–46}. Our group has reported that NTAs and their polymerizations tolerate mercaptans⁴⁷, alcohols⁴⁸, phenols⁴⁹ and water^{50,51}. Zhang et al. further proved that weak organic acid is not inhibitor or pollutant but catalyst of NTA polymerization⁵². The polymerization of β -amino acid NTAs was also found an effective way to synthesize β -peptides⁵³. However, NTAs with carboxyl groups are barely investigated^{54,55}, and their polymerizations have never been achieved to the best of our knowledge.

In this contribution, we synthesize two unprotected *N*-substituted NTAs (NNTAs), i.e., *N*-carboxypentyl glycine NTA (CPG-NTA) and iminodiacetic acid NTA (IDA-NTA) from aminocaproic acid and iminodiacetic acid both of which are extensively commercially available from industry. CPG-NTA shows good reactivity in the direct polymerization into polyCPGs with high MWs and low dispersities. On the contrary, instead of polymerization, IDA-NTA undergoes amidation of amine end group regio-selectively and transforms amines into carboxyl-ended species while hydroxyl groups keep intact. Detailed mechanism is further revealed by density functional theory (DFT) calculation. The polymerization of *N*-carboxybutyl glycine NTA (CBG-NTA) demonstrates that CPG-NTA is not an isolated case of polymerizable NNTA monomer with unprotected carboxyl groups. Physical property and pH-responsiveness of polyCPG are investigated and polyCPG serves as a good adhesive for various materials.

Results and discussion

Preparation and polymerization of CPG-NTA. Aminocaproic acid is extensively accessible by the hydrolysis of caprolactam and

recycled Nylon 6. Incorporation of aminocaproic acid as a sub-monomer into polypeptoids is an effective and noteworthy way to utilize it. From aminocaproic acid we successfully synthesize CPG and CPG-NTA (1 in Fig. 1a, Supplementary Fig. 1). CPG-NTA is characterized by ¹H nuclear magnetic resonance (¹H NMR, Supplementary Fig. 2a), ¹³C NMR (Supplementary Fig. 2b) and electrospray ionization mass spectra (ESI-MS, Supplementary Fig. 3). In its ¹H NMR spectrum, the signal ascribed to carboxylic acid proton is observed at the chemical shift of 11 ppm. Three carbon signals at 194.18, 179.50 and 165.04 ppm in ¹³C NMR indicate the existence of three carbonyl groups with various chemical environments rather than two typical carbonyl signals of other NNTAs reported⁴⁵. CPG-NTA with unprotected carboxyl groups is stable in purification and storage for months.

Direct polymerizations of CPG-NTA succeed without the protection on carboxyl group (Fig. 1a) as summarized in Table 1. *N,N*-dimethylacetamide (DMAc) is a good solvent for both acidic polymer and amine initiator which forms ammonium salt with monomer. Although it has been reported that polar solvents such as DMAc would hinder dethiocarboxylation of NTAs during polymerization⁵², we successfully carry out the homopolymerization of CPG-NTA in DMAc with relatively high yields of 72–91% (Samples 1–4). All polymerizations reach full conversion (>99%) except Sample 4 (97%) at the end of 2-day reaction. Degrees of polymerization (DPs) are predictable depending on the feed ratios of CPG-NTA and initiator. The MWs obtained from NMR (Fig. 1b) and SEC analyses (Fig. 1c) keep consistent and the dispersities (D_{SEC}) are lower than 1.12. Narrow symmetrical monomodal in size exclusion chromatography (SEC) traces of polyCPG products (Sample 1–4 in Fig. 1c) indicate good controllability of polymerization. When the feed ratio rises, slight decline of yield is observed, which is resulted from low concentration of amine, propagation reaction competed by impurities and side reaction in polar solvent. The polymerization is also examined in nonpolar solvent chloroform (Sample 5). The product, precipitated oligomer, is insoluble in chloroform due to pendant carboxyl groups and polymerization terminates at low conversion.

The products have been characterized by NMR and all signals in ¹H NMR and ¹³C NMR spectra (Fig. 1b and Supplementary Fig. 4) are fully assigned to the corresponding atoms of polyCPG. In ¹³C NMR spectrum (Supplementary Fig. 4), the signal of carboxylic acid is found at 174.60 ppm while those of amide backbone are observed at 169.24 ppm. The matrix-assisted laser desorption ionization-time of flight (MALDI-ToF) MS of polyCPG (Fig. 1e, f, Sample 3) shows a symmetric monomodal profile, which reveals neopentyl and amino end groups with CPG repeating units. In the zoom-in view (Fig. 1e), because of the substitution of proton of carboxyl group at the side chain by potassium cation, a series of weak peaks follow every major peak by a shift of 38 Da. The existence of massive carboxyl groups in polyCPG is thus confirmed. We successfully realize a direct polymerization of amino acid derivative bearing unprotected acidic pendant group.

CBG-NTA is another NNTA with unprotected carboxyl group (Supplementary Fig. 5, Supplementary Methods). The successful polymerization of CBG-NTA into polyCBG (Sample 6, Supplementary Figs. 6–8) demonstrate that CPG-NTA is not the only NNTA which is capable of polymerizing to acidic polypeptoids. Scientists can translate this system to other NNTAs with unprotected carboxyl groups.

To further investigate the polymerization behaviors of CPG-NTA and incorporate it into polymerizations of other amino acids, we carry out both random and block copolymerizations of CPG-NTA with NEG-NTA (Table 2). The random one produces poly(CPG-*r*-NEG) with composition close to the feed ratio and

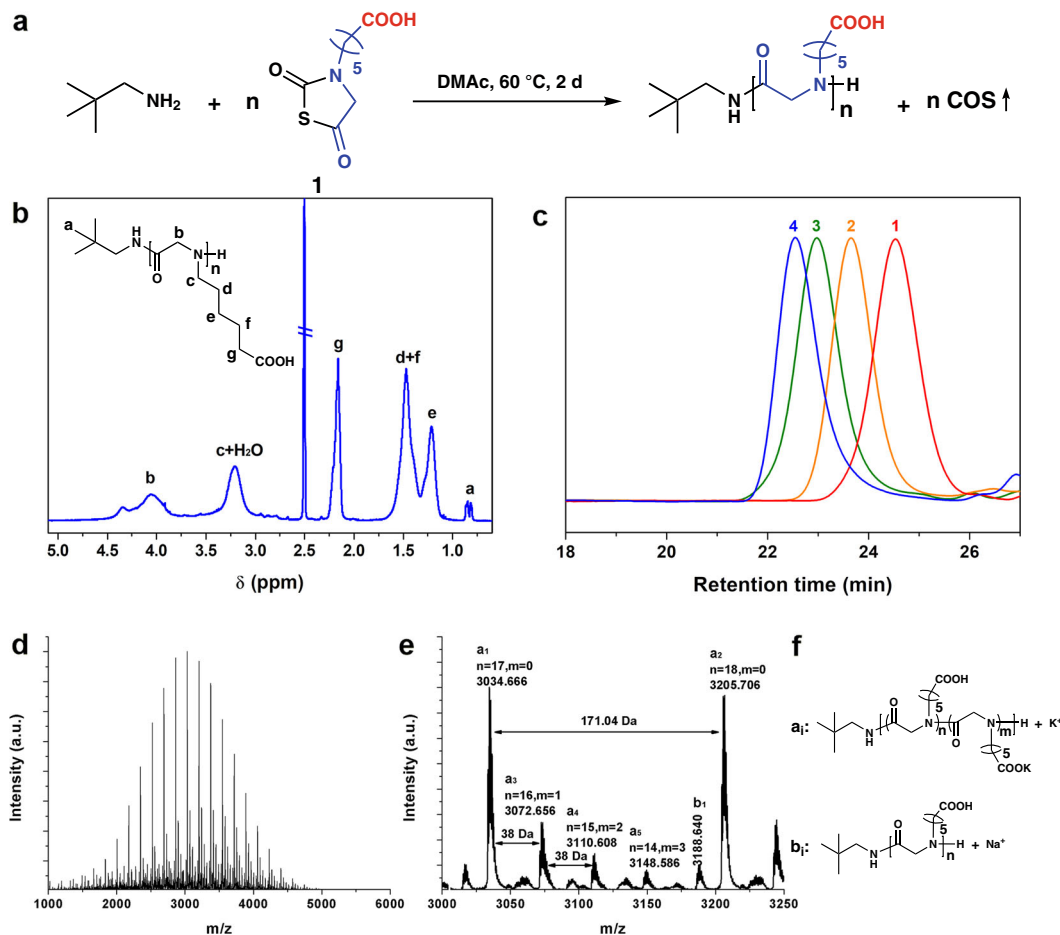


Fig. 1 Polymerization of CPG-NTA and characterization of polyCPGs. The scheme of CPG-NTA homo-polymerization and block copolymerization with NEG-NTA initiated by neopentylamine (a). ^1H NMR spectrum of polyCPG (Sample 3, // dimethyl sulfoxide (DMSO)) (b), SEC traces of product obtained from CPG-NTA polymerization (Samples 1–4) (c) and MALDI-ToF MS of polyCPG (Sample 2) (d) with the zoom-in view (e) and the corresponding chemical structures (f).

Table 1 Polymerization of CPG-NTA and CBG-NTA initiated by neopentylamine^a.

Sample	Monomer	$[\text{M}]_0/[\text{I}]_0$	Conv. %	Yield %	M_n theo ^b (kg mol^{-1})	DP_{NMR}^c	M_n NMR ^c (kg mol^{-1})	M_n SEC ^d (kg mol^{-1})	D_{SEC}^d
1	CPG-NTA	8	>99	91	1.3	8	1.5	2.8	1.12
2	CPG-NTA	20	>99	86	3.0	18	3.2	5.2	1.08
3	CPG-NTA	50	>99	84	7.3	45	7.8	7.8	1.09
4	CPG-NTA	70	97	73	8.9	58	10.0	9.3	1.09
5 ^e	CPG-NTA	20	39	30	1.1	7	1.3	2.6	1.09
6	CBG-NTA	20	>99	80	2.6	11	1.6	1.2	1.48

^a Polymerization conditions: $[\text{M}]_0 = 0.5 \text{ mol L}^{-1}$, 48 h at 60 °C in DMAc except Sample 5.

^b Number-average molecular weight (M_n) is calculated by $M_n \text{ theo} = [\text{M}]_0/[\text{I}]_0 \times \text{yield} \times \text{MW of repeat units} + \text{MW of initiator}$.

^c Determined by ^1H NMR.

^d Determined by SEC.

^e Polymerization conditions: $[\text{M}]_0 = 0.5 \text{ mol L}^{-1}$, 24 h at 58 °C in chloroform.

symmetrically monomodal SEC trace (Supplementary Fig. 9). By sequential feed of NEG-NTA and CPG-NTA monomers, poly (NEG-*b*-CPG) block copolymer is successfully obtained. The block polymerization reaches decent yield (>82%). The obvious peak shifts observed in SEC (Fig. 2a) from first block polymer indicate that most polyNEG chains are capable of further initiating the polymerization of CPG-NTA monomer in DMAc. Diffusion ordered spectroscopy spectrum (DOSY, Supplementary Fig. 10) of block copolymer (Sample 8) also excludes the existence of neither polyNEG nor polyCPG homopolymer. The structures of both copolymers are confirmed by ^1H NMR spectra (Fig. 2b,

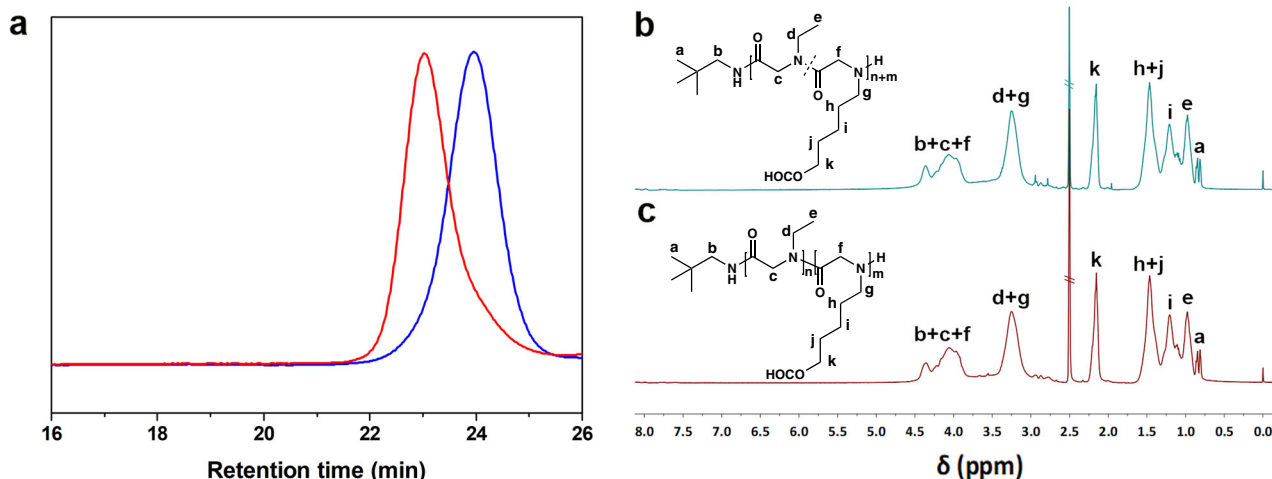
c). The success in preparation of copolymer of CPG-NTA reveals its ability to build complicated polymers for certain applications.

Preparation and polymerization of IDA-NTA. IDA is an easily accessible *N*-substituted glycine bearing two symmetrical carboxyl groups. Ester protected IDA-NTA has been synthesized to be bioactive gas donor⁵⁴. Taking advantage of its symmetric carboxyl groups, we successfully synthesize IDA-NTA (2 in Fig. 3a, Supplementary Fig. 11, Supplementary Methods) with high yields. It is characterized by ^1H NMR (Supplementary Fig. 12a),

Table 2 Copolymerization of CPG-NTA with NEG-NTA initiated by neopentylamine.

Sample	Feed molar ratio	Yield %	Polymer composition ^c	M_n SEC ^d (kg mol ⁻¹)	\bar{D}_{SEC} ^d
7 ^a	[CPG] ₀ /[NEG] ₀ /[I] ₀ = 18:20:1	83	poly(CPG ₁₉ - <i>r</i> -NEG ₂₀)	6.5	1.15
8 ^b	[NEG ^{1st}] ₀ /[CPG ^{2nd}] ₀ /[I] ₀ = 24:21:1	82	poly(NEG ₁₈ - <i>b</i> -CPG ₁₈)	4.9	1.15

^a Polymerization conditions: [M]₀ = 0.5 mol L⁻¹ in total, 48 h at 60 °C in DMAc.
^b Polymerization conditions: [M]₀ = 0.5 mol L⁻¹ for NEG-NTA and CPG-NTA, respectively at 60 °C in DMAc, 24 h for each block. Monomer molar equivalent amount of acetic acid is added to promote the polymerization.
^c Determined by ¹H NMR.
^d Determined by SEC.

**Fig. 2 Characterization of products obtained from block-copolymerization of CPG-NTA with NEG-NTA.** SEC traces **a** of first block polymer polyNEG (blue) and block copolymer poly(NEG-*b*-CPG) (Sample 8, red), and ¹H-NMR spectra of poly(CPG-*r*-NEG) (Sample 7) (**b**) and poly(NEG-*b*-CPG) (Sample 8) (**c**).

¹³C NMR (Supplementary Fig. 12b) and ESI-MS (Supplementary Fig. 13) spectra. Its ¹³C NMR and ¹H NMR spectra present three carbonyl signals and a signal of carboxyl proton at downfield, respectively, indicating the presence of unprotected carboxyl group similar to that in CPG-NTA.

Ring-opening reaction of IDA-NTA is investigated in various solvents (Fig. 3a, Samples 9–11 in Supplementary Table 1). Unlike CPG-NTA, the polymerization of IDA-NTA results in extremely low conversion of 4–10% in both nonpolar (Tetrahydrofuran (THF) and chloroform, Samples 9 and 10) and polar solvents (DMAc, sample 11). The ¹H NMR spectra and SEC traces (Supplementary Figs. 14 and 15) of the products (Sample 9 and 10) exclude the existence of polymer. Although the signals of IDA repeating units are found in the ¹H NMR spectrum of product precipitated from DMAc (sample 11, Supplementary Fig. 14c), the absence of polymer signal peak in its SEC trace (Supplementary Fig. 15) suggests only oligomerization of IDA-NTA. To figure out the reason behind the termination of IDA-NTA polymerization, we treat IDA-NTA with benzylamine at a feed ratio of 4 to analyze the chain end of oligoIDA obtained as a white powder. Four signals at 169.82, 167.18, 164.15 and 164.09 ppm in ¹³C NMR spectrum (Fig. 3b) are ascribed to four carbonyl groups. Moreover, two of them (Cⁱ and C^k) have very similar chemical environment indicating the existence of a six-membered ring composed of two identical *N*-substituted amide groups (3 in Fig. 3a). DP of IDA, 2.06, slightly higher than 2, is calculated by the integral ratio between IDA repeating units (H^{d+e+f+g}) and phenyl initiator residue (H^a) in ¹H NMR spectrum (Fig. 3c). The ESI-MS of product (Supplementary Fig. 16) confirms it as a cyclized IDA dimer capped by benzylamine. A small amount of species with a DP of 3 is also observed in ESI-MS indicating

overwhelming cyclization but propagation. The amidation reaction between amine and the carboxyl side group terminates propagation and transforms amine end groups into carboxyl end group with decent yield (89%) and quantitative conversion (99%) of benzylamine calculated from signal of amide proton (H^c) in Fig. 3c. The absence of signal ascribed to amine-ended species in ESI-MS (Supplementary Fig. 16) also confirms the full conversion of amines. The reaction between IDA-NTA and neopentylamine also results in the corresponding end-capped product with a precise DP of 2 characterized by NMR spectra (Supplementary Fig. 17).

PolyNEG₂₀ (Supplementary Table 1, sample 12) is applied to validate the effectiveness of IDA-NTA as a capping reagent to transform amines into carboxylic acids. Both the polyNEG macroinitiator and the isolated product are analyzed by MALDI-ToF MS in Fig. 3d–f. No obvious shift from polyNEG₂₀ to high MW is detected (Fig. 3d). In the zoom-in view (Fig. 3e), the disappearance of polyNEG (**a_n**) populations indicates the consumption of polyNEG by initiating ring-opening reaction of IDA-NTA. At the meantime, the populations with an *m/z* increase of 212 Da appear as **b_n** in the product spectrum. They are ascribed to polyNEG capped by 1,4-dicarboxymethylpiperazine-2,5-dione as a cyclic IDA dimer. The signals **c_n** with a shift of 38 Da from **b_n** provide evidence of potassium carboxylate end group converted from carboxylic acid.

Our previous work proves the tolerance of hydroxyl groups in NTA polymerizations. IDA-NTA termination is a regio-selective way to realize capping reaction of polymers or molecules to transform amine groups into carboxyl groups. The same capping reaction described is applied to 6-amino-1-hexanol resulting in high yield (99%). In ¹H and ¹³C NMR spectra (Supplementary Fig. 18), the proton and carbon signals of the methylene group

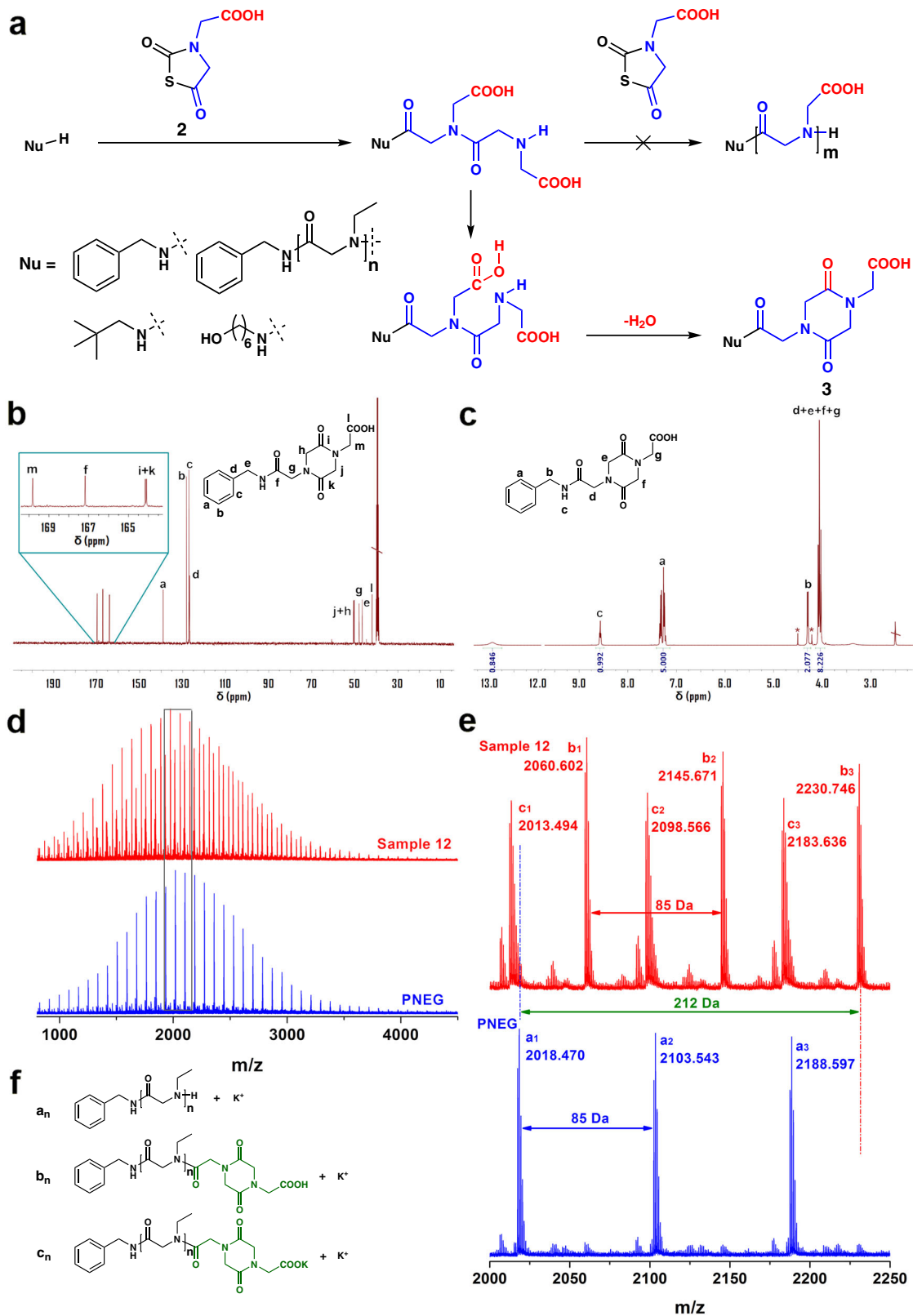


Fig. 3 Capping reaction of IDA-NTA and characterization of products. Scheme of reaction between IDA-NTA and benzylamine or polyNEG (**a**). ^{13}C NMR spectrum of product obtained from reaction between IDA-NTA and benzylamine with feed-ratio of 4 (**b**). ^1H NMR spectrum of product described above (\ DMSO, * IDA-NTA) (**c**). MALDI-ToF MS of macroinitiator polyNEG (blue) and product of reaction (red) in Sample 12, Supplementary Table 1 (**d**) with zoom-in views (**e**) and the corresponding chemical structures (**f**).

near hydroxyl group keep unchanged indicating the absence of capping reaction at the hydroxyl group. No ester group is detected supporting quantitative regio-selectivity of the capping reaction distinguishing amino group from hydroxyl one. The structure is also confirmed by ESI-MS (Supplementary Fig. 19) and no signal of amine-ended species is found. Instead of a monomer, IDA-NTA is demonstrated as an efficient regio-selective reagent to modify primary and secondary amino groups into carboxylic acids in one step with quantitative conversion. Though hydroxyl groups are common competent nucleophiles when using cyclic acid anhydride as capping reagent of amines, IDA-NTA approach has an advantage to tolerate them in the synthesis of carboxyl-ended functional polymers.

DFT calculation and NNTA with various linkers. DFT calculation is applied to figure out the difference between CPG-NTA and IDA-NTA polymerizations. All possible condensation routes of IDA (routes **A** and **A***) and CPG ends can be processed via two dehydration pathways, i.e., carbonyl addition-dehydration (routes **A**, **B** and **C**) and directly dehydration (routes **A***, **B*** and **C***) as shown in Supplementary Fig. 20 (Supplementary Data 1). The condensation of CPG end unit can occur with the last unit (route **B**) or the nearby one (**C**). Direct dehydration step, i.e., **A*** and **C*** are observed with lower ΔG in route **A** and **C** rather than carbonyl addition-dehydration steps since the formation of six- or ten-membered ring is enthalpy preferred as shown in Supplementary Table 2. Route **A*** for IDA end is confirmed with the lowest ΔG (37.6 kcal mol⁻¹) among the three, which indicates that IDA end group is proved with stronger tendency to dehydration than CPG with ΔG of 42.4 and 51.1 kcal mol⁻¹ (routes **B** and **C***).

NNTAs with intermediate-length linkers between CPG-NTA and IDA-NTA are checked. The successful polymerization of CBG-NTA (Sample 6) shows that NNTAs with unprotected carboxyl group can polymerize into the corresponding acidic polypeptoids. IDA-NTA is a special monomer in which the formation of six-member ring dimer prevents the polymerization according to experiments and calculation results. Unfortunately, we failed to synthesize *N*-carboxypropyl glycine NTA and *N*-carboxyethyl glycine NTA due to the competitive cyclization to seven- and six-member ring NNTAs, respectively. CPG-NTA is the best candidate to synthesize polypeptoids with pendant carboxyl groups among all checked NNTAs due to its good controllability and cheap origin.

Physical property and application of polyCPG. Thermogravimetric analysis (TGA) and differential scanning calorimetry (DSC) analyses have been applied to investigate the thermal property of polyCPG. The TGA trace (Supplementary Fig. 21) of polyCPG (Sample 3) shows that the decomposition temperature of 245 °C is close to that of other polypeptoids including polysarcosine and poly(*N*-butyl glycine)⁴⁵ because of the same amide backbones. In the DSC profiles (Fig. 4a) of polyCPG (Samples 2–4) with various DPs, three samples show glass transition temperatures (T_g s) of 19 °C, 54 °C and 43 °C, respectively. The melting temperatures (T_m s) among all profiles indicate crystal phase in polyCPG samples. T_m s of three samples are 160 °C, 152 °C and 168 °C with the corresponding melting enthalpies (ΔH_m s) of 3.21 J g⁻¹, 20.92 J g⁻¹ and 47.36 J g⁻¹, respectively. As DPs of polyCPGs increase, ΔH_m s rise obviously due to the growth of crystal phase in the polymer samples. A series of peak signals observed in XRD pattern of Sample 3 (Supplementary Fig. 22) further demonstrate that polyCPG crystallizes and forms ordered structures as other polypeptoids with long side chains³⁸.

The solubility of polyCPG is investigated by dissolving polyCPG (Sample 2) in various solvents (Supplementary Table 3,

Supplementary Methods). Due to the high polarity of carboxyl groups at the side chain, polyCPG is only able to dissolve in polar solvents including *N,N*-dimethylformamide (DMF), DMSO and alcohols, except acetonitrile and benzonitrile which are common solvents for many polypeptoids. Because of carboxyl groups, solubility of polyCPG in water is pH-responsive. A scan of solubility of polyCPG in water with different pHs by dynamic light scattering (DLS, Fig. 4b) shows that polyCPG dissolves well in alkali water giving very weak DLS signals. When pH decreases from 5 to 4.3, the solution turns turbid as polyCPG precipitates with irregular particle diameters. pH-responsiveness of polyCPG is a useful property for its further application in aqueous systems.

Due to amide backbone and carboxyl side groups, polyCPG samples are able to form hydrogen bonds between them or with other substances. While alkyl polypeptoids including polyNEG and polysarcosine show no adhesivity, the abundant hydrogen bonds enable polyCPG to serve as a surface adhesive material similar to other carboxyl group-containing polymers⁵⁶. PolyCPG powders and drops of water are deposited together on material surfaces and followed by rubbing or heating to activate the chain movement. It becomes pretty sticky to adhere two slices of substances together. Subsequent loss of solvent allows polyCPG to form a strong film between the two slices adhered (Fig. 4c). A weight of 1 kg can be hung under two slices of adhered poly(methyl methacrylate) (PMMA) after being dried overnight (Fig. 4e, inset image). We investigate the adhesion property of polyCPG by measuring the shear strength of the slices pulled slowly apart in the direction parallel to the adhered surfaces (Fig. 4c). The polypeptoid exhibits decent adhesive capability (33 to 229 kPa) to various materials including PMMA, stainless steel, wood and glass without chemical cross-linking (Fig. 4e). Figure 4d shows that pig skin tissue can be adhered immediately by polyCPG without being dried. The separated slices can be adhered again followed the methods described above and polyCPG is able to be recycled by washing it from slice surfaces with ethanol. PolyCPG is a promising candidate as a biocompatible adhesive material.

Methods

Synthesis of amino acids and NTAs. CPG hydrochloride were prepared according to the reported protocol⁵⁷. The prepared CPG hydrochloride (28.8 g, 0.1276 mmol) and *S*-ethoxythiocarbonyl mercaptoacetic acid (23.0 g, 0.1276 mol) were dissolved in 300 mL aqueous solution of NaOH (20.5 g, 0.5104 mol). The mixture was stirred for 3 days at room temperature. Then it was acidified by concentrated hydrochloric acid and extracted with ethyl acetate. The organic phase was washed with aqueous citric acid (5 wt%) and brine. The solvent was evaporated under reduced pressure after dried over Na₂SO₄. The concentrated liquid was purified by column (ethyl acetate: petroleum ether = 1:2) and a white powder was obtained by recrystallization in ethanol and water (7.2 g, 2.596 mmol). Then the powder was dissolved in 300 mL ethyl acetate. 4.5 mL PBr₃ (about 12.7 g, 0.0469 mmol) was added dropwise to the solution in 0 °C ice bath in 15 min. After stirred for 1 h at room temperature, the mixture was washed by water and brine for 3 times, respectively, and then dried over MgSO₄. A white powder was obtained by recrystallization in ethyl acetate and petroleum ether (4.7 g, yield 16%) and to be stored under an argon atmosphere.

The synthesis of CBG-NTA and IDA-NTA followed similar procedure described above. The experimental details and monomers characterization are included in Supplementary Methods.

Polymerization of NTAs. All polymerizations and end-capping reactions were carried out using Schlenk technique, and all reaction vials were flame dried and purged with argon.

As a typical polymerization, CPG-NTA (170.2 mg, 0.7359 mmol) was dissolved in 1.2 mL DMAc followed by 0.28 mL neopentylamine solution in DMAc (0.05208 mmol mL⁻¹). The reaction was carried out at 60 °C for 48 h. After precipitation from diethyl ether and centrifugation, the product was collected and dried under vacuum to a constant weight (107 mg, 84%).

As a typical polymerization or end-capping reaction of IDA-NTA, IDA-NTA (0.3098 g, 1.815 mmol) was dissolved in 2.8 mL THF followed by 0.50 mL benzylamine solution in THF (0.1812 mmol mL⁻¹). It was incubated in 60 °C for 24 h. After precipitation from diethyl ether and centrifugation, the product was dried under vacuum to constant weight (9 mg, 4%).

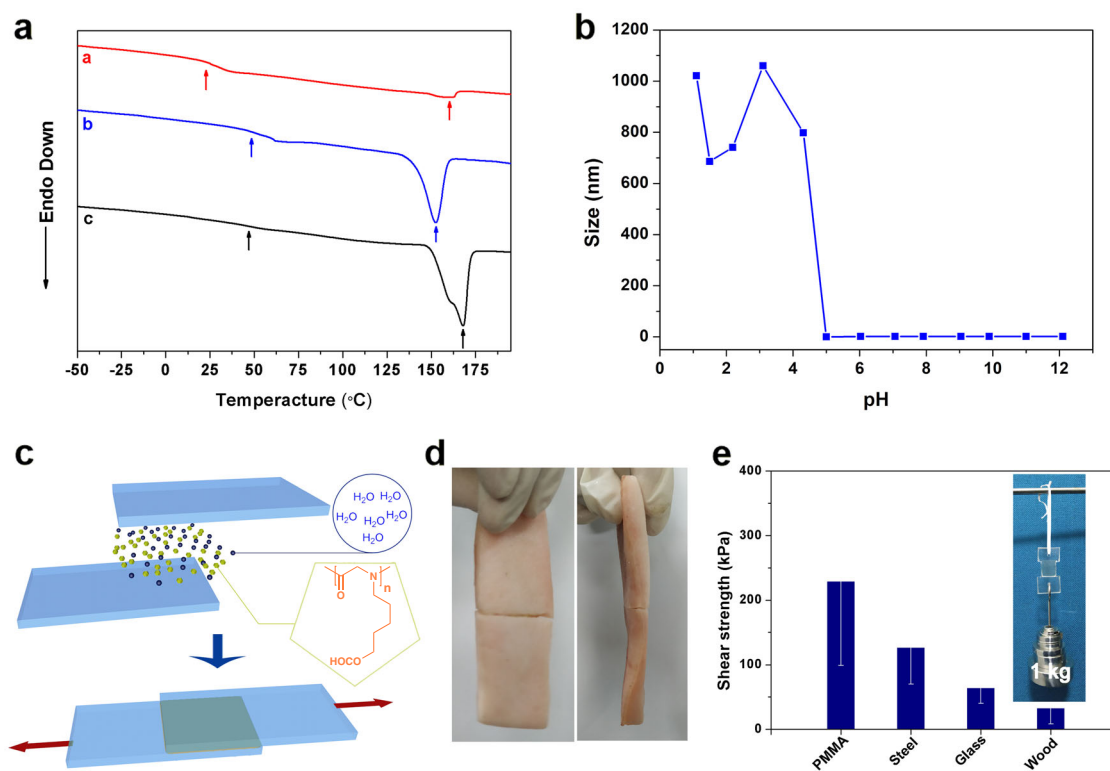


Fig. 4 Physical property test and adhesion experiment of polyCPGs. DSC profiles of Samples 2 (a, red) 3 (b, blue) and 4 (c, black) (a). pH-responsive solubility of polyCPG (Sample 2) in water (b). Illustration of adhesion procedure (c). Adhesion experiment of polyCPG on swine skin tissue (d). Shear strength of polyCPGs on different materials (e). The inset image illustrates the adhesive behavior of polyCPGs on PMMA.

Adhesive experiment. A polyCPG sample (25 mg) was deposited on a slice with a 20 mm × 20 mm area followed by 20 μ L deionized water. By rubbing the polymer swelled with another slice, they were adhered. The samples were let stand still overnight at room temperature to dry before tensile measurement except adhered swine skin tissue. The slices were drawn by tensile tester in the direction parallel to the adhered surface at a rate of 5 mm min⁻¹. The shear strength was calculated from the maximum force divided by the area of adhered surface. The experiments for every material are repeated for three times and standard errors are calculated.

Calculation details. All geometries of transition states (TSs) and intermediates were optimized under tight criteria using M06-2X⁵⁸/6-31G(d,p) with DFT-D3 correction⁵⁹. Frequency calculations were employed to confirm that the intermediates and TSs had zero and one imaginary frequency, respectively. The reaction pathway of all TS was checked by intrinsic reaction coordinate (IRC)⁶⁰. Thermal correction to Gibbs free energies was obtained at 298.2 K and 1.013 × 10⁵ Pa. All calculations were performed using Gaussian 16 program as we reported before^{61–63}.

Data availability

The data used in this study are available from the corresponding authors upon reasonable request.

Received: 5 August 2020; Accepted: 29 September 2020;

Published online: 28 October 2020

References

- Bartlett, G. J., Porter, C. T., Borkakoti, N. & Thornton, J. M. Analysis of catalytic residues in enzyme active sites. *J. Mol. Biol.* **324**, 105–121 (2002).
- Parales, R. E. et al. Substrate specificity of naphthalene dioxygenase: effect of specific amino acids at the active site of the enzyme. *J. Bacteriol.* **182**, 1641–1649 (2000).
- Vallee, B. L. & Auld, D. S. Active-site zinc ligands and activated H₂O of zinc enzymes. *Proc. Natl Acad. Sci. USA* **87**, 220–224 (1990).
- Galhoum, A. A. et al. Aspartic acid grafting on cellulose and chitosan for enhanced Nd(III) sorption. *React. Funct. Polym.* **113**, 13–22 (2017).
- Tian, C., Ling, J. & Shen, Y. Q. Self-assembly and pH-responsive properties of poly(L-glutamic acid-r-L-leucine) and poly(L-glutamic acid-r-L-leucine)-b-polysarcosine. *Chin. J. Polym. Sci.* **33**, 1186–1195 (2015).
- Chen, C. Y., Lin, M. S. & Hsu, K. R. Recovery of Cu(II) and Cd(II) by a chelating resin containing aspartate groups. *J. Hazard. Mater.* **152**, 986–993 (2008).
- Karal-Yilmaz, O. et al. Synthesis and characterization of poly(L-lactic acid-co-ethylene oxide-co-aspartic acid) and its interaction with cells. *J. Mater. Sci.* **17**, 213–227 (2006).
- Bajaj, I. & Singhal, R. Poly (glutamic acid)—an emerging biopolymer of commercial interest. *Bioresour. Technol.* **102**, 5551–5561 (2011).
- Lollo, G. et al. Polyglutamic acid-PEG nanocapsules as long circulating carriers for the delivery of docetaxel. *Eur. J. Pharm. Biopharm.* **87**, 47–54 (2014).
- Arroyo-Crespo, J. J. et al. Anticancer activity driven by drug linker modification in a polyglutamic acid-based combination-drug conjugate. *Adv. Funct. Mater.* **28**, 1800931 (2018).
- Zhou, Y. et al. Polyaniline-loaded gamma-polyglutamic acid nanogels as a platform for photoacoustic imaging-guided tumor photothermal therapy. *Nanoscale* **9**, 12746–12754 (2017).
- Raj, M. & Goyal, R. N. A poly-(melamine)/poly-(glutamic acid) based electrochemical sensor for sensitive determination of 2-Thioxanthine. *Sens. Actuat. B* **250**, 552–562 (2017).
- Xia, J. et al. Polyglutamic acid based polyanionic shielding system for polycationic gene carriers. *Chin. J. Polym. Sci.* **34**, 316–323 (2016).
- Tao, Y. et al. Synthesis and properties of alternating polypeptides and polyampholytes as protein-resistant polymers. *Biomacromolecules* **19**, 936–942 (2018).
- Ni, Y. et al. Two-dimensional supramolecular assemblies from pH-responsive poly (ethyl glycol)-b-poly (l-glutamic acid)-b-poly (N-octylglycine) triblock copolymer. *Biomacromolecules* **18**, 3367–3374 (2017).
- Zheng, J. et al. pH-sensitive poly(glutamic acid) grafted mesoporous silica nanoparticles for drug delivery. *Int. J. Pharm.* **450**, 296–303 (2013).
- Zhang, C. et al. From neutral to zwitterionic poly (α -amino acid) nonfouling surfaces: Effects of helical conformation and anchoring orientation. *Biomaterials* **178**, 728–737 (2018).

18. Zhang, C. et al. Investigation on the linker length of synthetic zwitterionic polypeptides for improved nonfouling surfaces. *ACS Appl. Mater. Interfaces* **10**, 17463–17470 (2018).
19. Zimpel, A. et al. Coordinative binding of polymers to metal-organic framework nanoparticles for control of interactions at the biointerface. *ACS Nano* **13**, 3884–3895 (2019).
20. Sun, Y. et al. Conformation-directed formation of self-healing diblock copolypeptide hydrogels via polyion complexation. *J. Am. Chem. Soc.* **139**, 15114–15121 (2017).
21. Ji, S. et al. Light-and metal ion-induced self-assembly and reassembly based on block copolymers containing a photoresponsive polypeptide segment. *Macromolecules* **52**, 4686–4693 (2019).
22. Nishimura, T., Hirose, S., Sasaki, Y. & Akiyoshi, K. Substrate-sorting nanoreactors based on permeable peptide polymer vesicles and hybrid liposomes with synthetic macromolecular channels. *J. Am. Chem. Soc.* **142**, 154–161 (2020).
23. Sternhagen, G. L. et al. Solution self-assemblies of sequence-defined ionic peptoid block copolymers. *J. Am. Chem. Soc.* **140**, 4100–4109 (2018).
24. Lau, K. H. et al. Self-assembly of ultra-small micelles from amphiphilic lipopeptides. *Chem. Commun.* **53**, 2178–2181 (2017).
25. Lau, K. H. et al. Molecular design of antifouling polymer brushes using sequence-specific peptoids. *Adv. Mater. Interfaces* **2**, 1400225 (2015).
26. Birke, A., Ling, J. & Barz, M. Polysarcosine-containing copolymers: synthesis, characterization, self-assembly, and applications. *Prog. Polym. Sci.* **81**, 163–208 (2018).
27. Robertson, E. J. et al. Design, synthesis, assembly, and engineering of peptoid nanosheets. *Acc. Chem. Res.* **49**, 379–389 (2016).
28. Huesmann, D., Klinker, K. & Barz, M. Orthogonally reactive amino acids and end groups in NCA polymerization. *Polym. Chem.* **8**, 957–971 (2017).
29. Bai, T. & Ling, J. Polymerization rate difference of N-alkyl glycine NCAs: steric hindrance or not? *Biopolymers* **110**, e23261 (2019).
30. Vacogne, C. D., Wei, C., Tauer, K. & Schlaad, H. Self-Assembly of α -helical polypeptides into microscopic and enantiomeric spirals. *J. Am. Chem. Soc.* **140**, 11387–11394 (2018).
31. Hanay, S. B. et al. Facile approach to covalent copolypeptide hydrogels and hybrid organohydrogels. *ACS Macro Lett.* **7**, 944–949 (2018).
32. Wan, Y. et al. pH-responsive peptide supramolecular hydrogels with antibacterial activity. *Langmuir* **33**, 3234–3240 (2017).
33. Yuan, J. et al. Salt- and pH-triggered helix-coil transition of ionic polypeptides under physiology conditions. *Biomacromolecules* **19**, 2089–2097 (2018).
34. Wollenberg, A. et al. Injectable polypeptide hydrogels via methionine modification for neural stem cell delivery. *Biomaterials* **178**, 527–545 (2018).
35. Sun, Y. & Deming, T. J. Self-Healing multiblock copolypeptide hydrogels via polyion complexation. *ACS Macro Lett.* **8**, 553–557 (2019).
36. Gazon, C. et al. Aqueous ring-opening polymerization-induced self-assembly (ROPISA) of N-carboxyanhydrides. *Angew. Chem. Int. Ed.* **59**, 622–626 (2020).
37. Zuckermann, R. N. Peptoid origins. *Pept. Sci.* **96**, 545–555 (2011).
38. Greer, D. R. et al. Universal relationship between molecular structure and crystal structure in peptoid polymers and prevalence of the cis backbone conformation. *J. Am. Chem. Soc.* **140**, 827–833 (2018).
39. Sun, J. et al. Self-assembly of crystalline nanotubes from monodisperse amphiphilic diblock copolypeptide tiles. *Proc. Natl Acad. Sci. USA* **113**, 3954–3959 (2016).
40. Lavilla, C. et al. Block-sequence-specific glycopolypeptides with selective lectin binding properties. *Biomacromolecules* **18**, 1928–1936 (2017).
41. Barz, M., Duro-Castano, A. & Vicent, M. J. A versatile post-polymerization modification method for polyglutamic acid: synthesis of orthogonal reactive polyglutamates and their use in “click chemistry”. *Polym. Chem.* **4**, 2989 (2013).
42. Nakanishi, M. et al. Study of the quantitative aminolysis reaction of poly(β -benzyl l-aspartate) (PBLA) as a platform polymer for functionality materials. *React. Funct. Polym.* **67**, 1361–1372 (2007).
43. Cao, J. et al. Interfacial ring-opening polymerization of amino-acid-derived N-thiocarboxyanhydrides toward well-defined polypeptides. *ACS Macro Lett.* **6**, 836–840 (2017).
44. Tao, X., Zheng, B., Kricheldorf, H. R. & Ling, J. Are N-substituted glycine N-thiocarboxyanhydride monomers really hard to polymerize? *J. Polym. Sci. Part A* **55**, 404–410 (2017).
45. Tao, X., Deng, Y., Shen, Z. & Ling, J. Controlled polymerization of N-substituted glycine N-thiocarboxyanhydrides initiated by rare Earth borohydrides toward hydrophilic and hydrophobic polypeptides. *Macromolecules* **47**, 6173–6180 (2014).
46. Tao, X., Du, J., Wang, Y. & Ling, J. Polypeptides with tunable cloud point temperatures synthesized from N-substituted glycine N-thiocarboxyanhydrides. *Polym. Chem.* **6**, 3164–3174 (2015).
47. Tao, X. et al. Polymerization of N-substituted glycine N-thiocarboxyanhydride through regioselective initiation of cysteamine: a direct way toward thiol-capped polypeptides. *Macromolecules* **51**, 4494–4501 (2018).
48. Tao, X. et al. Hydroxyl group tolerated polymerization of N-substituted glycine N-thiocarboxyanhydride mediated by sminoalcohols: a simple way to α -hydroxyl- ω -aminotelechelic polypeptides. *Macromolecules* **50**, 3066–3077 (2017).
49. Miao, Y. et al. Fe³⁺@polyDOPA-b-polysarcosine, a T1-weighted MRI contrast agent via controlled NTA polymerization. *ACS Macro Lett.* **7**, 693–698 (2018).
50. Zheng, B. et al. Identifying the hydrolysis of carbonyl sulfide as a side reaction impeding the polymerization of N-substituted glycine N-thiocarboxyanhydride. *Biomacromolecules* **19**, 4263–4269 (2018).
51. Zheng, B., Tao, X. & Ling, J. Water tolerated polymerization of N-substituted glycine N-thiocarboxyanhydride initiated by primary amines. *Acta Polym. Sin.* **0**, 72–79 (2018).
52. Siefker, D., Williams, A. Z., Stanley, G. G. & Zhang, D. Organic acid promoted controlled ring-opening polymerization of α -amino acid-derived N-thiocarboxyanhydrides (NTAs) toward well-defined polypeptides. *ACS Macro Lett.* **7**, 1272–1277 (2018).
53. Zhou, M. et al. Water-insensitive synthesis of poly- β -peptides with defined architecture. *Angew. Chem. Int. Ed.* **59**, 7240–7244 (2020).
54. Powell, C. R. et al. Functional N-substituted N-thiocarboxyanhydrides as modular tools for constructing H₂S donor conjugates. *ACS Chem. Biol.* **14**, 1129–1134 (2019).
55. Miyamoto, T. et al. Agonistic action of synthetic analogues of quisqualic acid at the insect neuromuscular junction. *Arch. Insect Biochem. Physiol.* **2**, 65–73 (1985).
56. Qi, Z. et al. Exploring a naturally tailored small molecule for stretchable, self-healing, and adhesive supramolecular polymers. *Sci. Adv.* **4**, eaat8192 (2018).
57. Gibbs, T. J. K., Boomhoff, M. & Tomkinson, N. C. O. A mild and efficient method for the one-pot monocarboxymethylation of primary amines. *Synlett.* 1573–1576 (2007).
58. Zhao, Y. & Truhlar, D. G. The M06 suite of density functionals for main group thermochemistry, thermochemical kinetics, noncovalent interactions, excited states, and transition elements: two new functionals and systematic testing of four M06-class functionals and 12 other functionals. *Theor. Chem. Acc.* **120**, 215–241 (2008).
59. Grimme, S., Antony, J., Ehrlich, S. & Krieg, H. A consistent and accurate ab initio parametrization of density functional dispersion correction (DFT-D) for the 94 elements H–Pu. *J. Chem. Phys.* **132**, 154104 (2010).
60. Fukui, K. The path of chemical reactions—the IRC approach. *Acc. Chem. Res.* **14**, 363–368 (1981).
61. Frisch, M. J. et al. Gaussian 16 Rev. B.01 (Gaussian, Inc., Wallingford, CT, 2016).
62. Bai, T. W., Ni, X. F., Ling, J. & Shen, Z. Q. Mechanism of Janus polymerization: a DFT study. *Chin. J. Polym. Sci.* **37**, 990–994 (2019).
63. Bai, T. W. & Ling, J. NAM-TMS mechanism of alpha-amino acid N-carboxyanhydride polymerization: a DFT study. *J. Phys. Chem. A* **121**, 4588–4593 (2017).

Acknowledgements

This work is financially supported by the National Natural Science Foundation of China (21674091, 81971600, 81871403) and Key Research and Development Program of Zhejiang Province (2019C03014).

Author contributions

J.L., J.S. and B.Z. conceived the project and designed the experimental procedures. B.Z. carried out the experiments and analyzed data. T.B. performed the DFT calculation to elucidated the mechanism. J.L. and J.S. supervised the execution of the experiments and data analysis. B.Z. drafted the paper with contribution from J.L., J.S. and T.B. All authors reviewed the final paper.

Competing interests

The authors declare no competing interests.

Additional information

Supplementary information is available for this paper at <https://doi.org/10.1038/s42004-020-00393-y>.

Correspondence and requests for materials should be addressed to J.L. or J.S.

Reprints and permission information is available at <http://www.nature.com/reprints>

Publisher's note Springer Nature remains neutral with regard to jurisdictional claims in published maps and institutional affiliations.



Open Access This article is licensed under a Creative Commons Attribution 4.0 International License, which permits use, sharing, adaptation, distribution and reproduction in any medium or format, as long as you give appropriate credit to the original author(s) and the source, provide a link to the Creative Commons license, and indicate if changes were made. The images or other third party material in this article are included in the article's Creative Commons license, unless indicated otherwise in a credit line to the material. If material is not included in the article's Creative Commons license and your intended use is not permitted by statutory regulation or exceeds the permitted use, you will need to obtain permission directly from the copyright holder. To view a copy of this license, visit <http://creativecommons.org/licenses/by/4.0/>.

© The Author(s) 2020